GEOPHYSICS, VOL. 33, NO. 6 (DECEMBER 1968), P. 972-979, 12 FIGS., 5 TABLES

THE INVERSE PROBLEM OF MAGNETOTELLURIC SOUNDING†

FRANCIS T. WU*

Based on the model of a flat layered earth, a nonlinear, least-squares method is used to invert magnetotelluric sounding curves to obtain the layer resistivities and thicknesses. Partial derivatives of the apparent resistivity with respect to layer parameters show the manner in which the layer parameters are contributing to the apparent resistivities. Uniqueness of the inversion is not guaranteed, but when the partial derivatives are linearly independent and the relative magnitudes of the layer resistivities of the initial guess are not too far from the correct ones, the convergence of the method to the correct values seems to be ensured.

INTRODUCTION

The magnetotelluric sounding (MTS) method has been used extensively in exploration geophysics for a number of years in this country and in Europe (Vozoff et al, 1964). This same method, though in a different frequency range, has been used to deduce subsurface geophysical information in addition to that obtained by seismic, gravity, and/or heat flow surveys (Cantwell and Madden, 1960; Swift, 1967). The MTS results, being of somewhat different nature from those of seismic, gravity, and heat flow, would certainly reveal more about the crust and the upper mantle. In particular, as the earth material consists mainly of semiconductors, the electrical conductivity would have a strong dependence on temperature; we can thus gain one more control over the temperature in the earth.

Interpretation of MTS data in the past was mostly done by trial and error or master-curve matching. Two-layer and three-layer master curves were published by Cagniard (1953) and Yungul (1961). The trial and error method could be very painstaking, especially when a large number of parameters are involved, and the curve-matching technique is very limited in resolution. With the general availability of electronic computers and better matched recording equipment, it is possible and desirable to invert the data automatically to save time and to attain maximum use of the data.

MTS interpretation is complicated mainly by two factors: the source of the electromagnetic wave and the geological conditions. The source may be of finite horizontal dimension so that for different frequencies the nature of the incident EM wave would be dissimilar. The problem has been investigated by Wait (1954) and Price (1962). However, the assumptions made by Cagniard in his classical paper are valid in many cases (Madden and Nelson, 1964). Geologically, the lateral variation might be so severe that the situation cannot be adequately described by a system of parallel layers in the case of a flat earth approximation, or by concentric layers in the case of a spherical earth. The crust of the earth is expected to be very nonhomogeneous; with increasing depth, the lateral variation is expected to diminish. In order to avoid this complication, we have to choose the recording sites carefully.

In this paper we will use the flat-layered half-space for our model. This model is justified when the skin-depth effect of the waves is small compared to the radius of the earth. When the necessity arises, one has only to change to a spherical model. The inversion method is quite general.

Under the assumption of a plane-wave incident upon a layered half-space, the calculation by apparent resistivity as a function of layer resistivity and thickness can easily be achieved (Cagniard, 1953; Vozoff, 1958). For computer calculation one can easily apply the Thomson-Haskell matrix method (Haskell, 1953). The definition of

† Contribution No. 1514, Division of Geological Sciences, California Institute of Technology, Pasadena, California. Manuscript received by the Editor January 29, 1968; revised manuscript received July 22, 1968.

* California Institute of Technology, Pasadena, California; now with Weston Observatory, Boston College, Chestnut Hill, Massachusetts.

various parameters and the general geometry are included in Figure 1. In this paper we assume that ρ is expressed in ohm meters and h in kilometers.

THE INVERSE PROBLEM

When the source and geological conditions permit the Cagniard model to be a valid representation, it is desirable to find the parameters rapidly, usually the resistivities and the thicknesses, of the layers and obtain some assessment as to the accuracy of the estimate. Even with the high-speed computers now available, the prevalent trial and error method of finding the set of parameters which yields the best fitting curve is a tedious and sometimes arbitrary process. In fact, at present, most of the data interpretation involves matching of master curves based on two-layered or three-layered models. We can however use the combination of a least-squares method and an iteration scheme to perform the modification of initial model automatically. Thus it is possible to use models with many layers to obtain faster and better solutions.

The basic principles of least-square methods can be found in Margenau and Murphy (1943). We shall outline the method as applied to magnetotelluric sounding. Let ρ_{ci} be the calculated apparent resistivity and ρ_{0i} be the observed resistivity at period T_i. We wish to satisfy the least-squares condition

$$\Phi = \sum_i (\rho_{ci} - \rho_{0i})^2 = \text{a minimum.}$$

We can write ρ_{ci} as

$$\rho_{ci} = f(\rho_1, \rho_2 \cdots \rho_n, h_1, h_2 \cdots h_n; T_i).$$

For a small change in one of the parameters, there will be a corresponding change of ρ_{ci}. We use the approximation

$$\frac{\partial \rho_{ci}}{\partial \rho_j} \cong \frac{\Delta \rho_{ci}}{\Delta \rho_j} = \frac{1}{\Delta \rho_j} f(\rho_1, \rho_2, \cdots, \rho_j + \Delta \rho_j, \cdots, \rho_n, h_1, h_2 \cdots h_n; T_i). \tag{1}$$

Similar relations exist for h_i's. Then we can write, to first order,

$$d\rho = \rho_{0i} - \rho_{ci} = \frac{\partial \rho_{ci}}{\partial \rho_1} d\rho_1 + \cdots \frac{\partial \rho_{ci}}{\partial \rho_n} d\rho_n + \frac{\partial \rho_{ci}}{\partial h_1} dh_1 + \cdots + \frac{\partial \rho_{ci}}{\partial h_n} dh_n \tag{2}$$

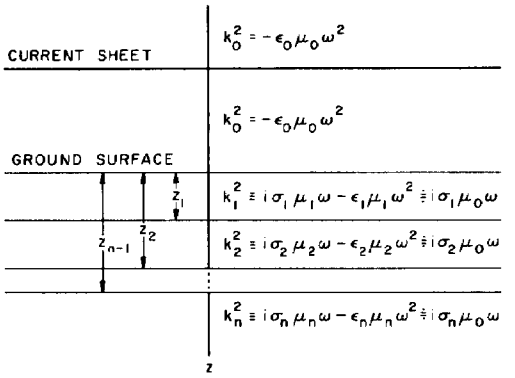

FIG. 1. Geometry of the problem.

for each i. If we define

$$D = (d\rho_1, \cdots, d\rho_n, dh_1 \cdots dh_n),$$

$$P = \begin{vmatrix} \frac{\partial \rho_{c1}}{\partial \rho_1} & \cdots & \frac{\partial \rho_{c1}}{\partial h_n} \\ \cdot & & \cdot \\ \cdot & & \cdot \\ \frac{\partial \rho_{ck}}{\partial \rho_1} & \cdots & \frac{\partial \rho_{cn}}{\partial h_n} \end{vmatrix} \tag{3}$$

$$R = (\rho_{01} - \rho_{c1}, \rho_{02} - \rho_{c2}, \cdots, \rho_{0k} - \rho_{ck}\chi);$$

we have

$$PD = R.$$

We can then solve for D from

$$D = (P^T P)^{-1} P^T R, \tag{4}$$

where the superscript T denotes the transpose operation. These are the normal equations corresponding to the condition

$$\frac{\partial \Phi}{\partial (d\rho_i)} = 0.$$

However, f is nonlinear in ρ and h and neglecting higher order derivatives may not ensure the achievement of a least-squares condition if the magnitude of vector D is large. Several iterations are generally needed for convergence of Φ to a limit.

For our numerical calculations, we have chosen to use a procedure, devised by Marquardt (1963), in which the step size and the direction of the correction vector are determined simultaneously to insure proper convergence.

Uniqueness is not guaranteed in this method.

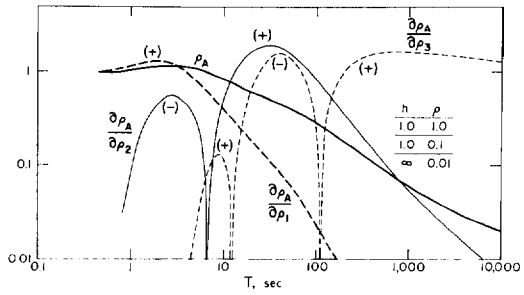

FIG. 2. Apparent resistivity and partial derivative curves for model (1). The signs of the partial derivative are indicated by the + and − signs adjacent to the curves.

PARTIAL DERIVATIVES

Partial derivatives are used in the inversion scheme we described in the last section. Because of the finite conductivity of the earth, EM waves at different periods suffer different degrees of attenuation. At very short periods with corresponding skin depth smaller than layer thickness, the energy is almost guided along the surface; hence only a change in uppermost layer conductivity would affect wave amplitude, i.e., $\partial\rho_A/\partial\rho_1 = 1$ and $\partial\rho_A/\partial h_1$, $\partial\rho_A/\partial\rho_2$ and so on would all be zero. At longer periods, the energy is distributed in different layers in different amounts; the way in which the partial derivatives behave depends on the skin depth and layer thicknesses. Calculation of these derivatives can either be done by analytical differentiation or a numerical, finite-difference method. We found that in the case of MTS the second method is faster, and if the increment is small enough, the accuracy is very good. In Figures 2, 3, and 4 we have presented the partial derivatives for three typical cases: (1) decreasing resistivity downward (Figure 2), (2) increasing resistivity downward (Figure 3), and (3) with a layer of low resistivity in between (Figure 4). These demonstrate clearly the general characteristics of the partial curves. The apparent resistivity at a certain period can be viewed as a weighted average of the layer resistivity. In this respect it resembles the dispersion curve of surface waves where the velocity at a certain period is a weighted average of the layer compressional and shear velocities. The partial derivatives have been used successfully to interpret the surface wave dispersion data (Anderson, 1966), and inversion of such data has been attempted by Dorman and Ewing (1962), Archambeau and Anderson (1963), and more recently Backus and Gilbert (1967).

In cases (1) and (3), $\partial\rho_A/\partial\rho_1$ are severely attenuated toward zero for long periods reflecting the condition that the top layer is relatively transparent to EM waves at longer periods at which the energy concentrates in the lower layers. For model (2), however, $\partial\rho_A/\partial\rho_1$ increases with increasing period until 2000 sec; from there on, it decreases very gradually: the curve follows fairly closely the trend of the ρ_A curve. This phenomenon means that the first layer is rather translucent, and when ρ_1 is increased, it becomes more transparent, thus enabling us to see the lower layers at shorter periods.

The general features of $\partial\rho_A/\partial\rho_2$ are that there are places where $\partial\rho_A/\partial\rho_2$ has zeros and changes signs across the zeros, and at very long periods and very short periods it tends to zero. Whereas $\partial\rho_A/\partial\rho_1$ has as a rule a value of 1 for $T\to 0$, $\partial\rho_A/\partial\rho_2$ has diverse values depending on the layer resistivity: the higher the layer resistivity, the smaller $\partial\rho_A/\partial\rho_2$. These properties are in fact common for all the internal layers as shown in

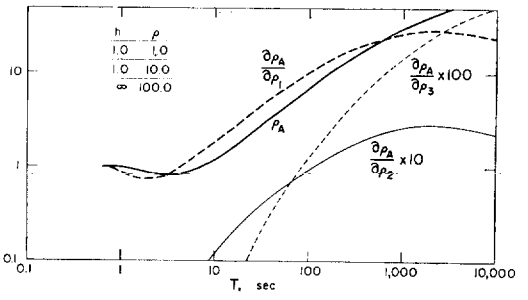

FIG. 3. Apparent resistivity and layer resistivity partial derivative curves for model (2).

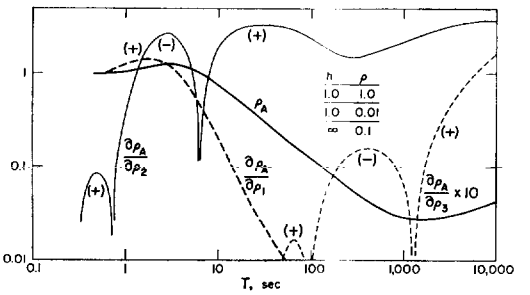

FIG. 4. Apparent resistivity and layer resistivity partial derivative curves for model (3).

Figure 5. The parameters of the layered medium are quoted from a paper by Vozoff et al (1964). $\partial\rho_A/\partial\rho_4$ is in the numerical noise of the computation and is omitted. $\partial\rho_A/\partial\rho_2$ and $\partial\rho_A/\partial\rho_3$ have similar shapes; although $\partial\rho_A/\partial\rho_3$ is more than an order of magnitude larger than $\partial\rho_A/\partial\rho_2$. It becomes clear at this point that a layer of high resistivity in a system of low resistivity layers will be very difficult to detect.

$\partial\rho_A/\partial\rho_3$ curves in Figures 2, 3, and 4 show the tendency to approach 1 as T becomes very large. This is the result of the very large penetration depth of signals of very long periods at which $\rho_A \to \rho_3$ and $\partial\rho_A/\partial\rho_3 \to 1$. This conclusion is true for the half-space in any layered system (cf. Figure 5).

$\partial\rho_A/\partial h$ curves presented in Figures 6 and 7 have much the same character as $\partial\rho_A/\partial\rho$'s for the internal layers. For small T and large T, $\partial\rho_A/\partial h$ tends to 0, for the same reason that $\partial\rho_A/\partial\rho_2$ tends to 0. Namely very short-period waves would not "feel" the effect of the changes in the layer thickness because of small skin depth, on the other hand, at extremely long periods, the half-space resistivity is the only deciding factor.

For the problem of uniqueness of inversion mentioned in the last section, the partial derivatives seem to offer a necessary condition: if the partial derivatives are not linearly independent of each other, the inversion could not be unique. We would also expect the uniqueness to be rather local, i.e., if the initial guesses, or at least their relative magnitudes, are not too far off from the correct values. And insofar as we are using numerical methods to invert, we would further expect the resistivity of the layers with very small partial derivatives to be badly determined, since the effect of these layers might be buried in the numerical noise.

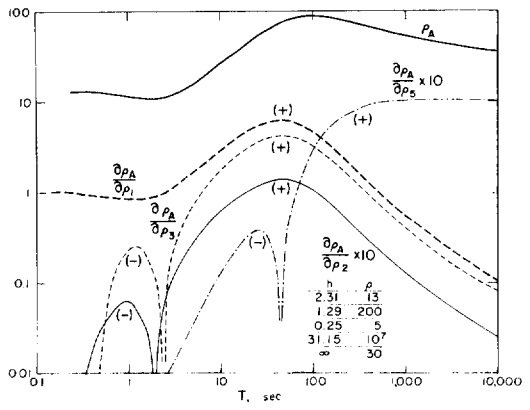

FIG. 5. Apparent resistivity and layer resistivity partial derivative curves for the five layer model of Vozoff et al (see text).

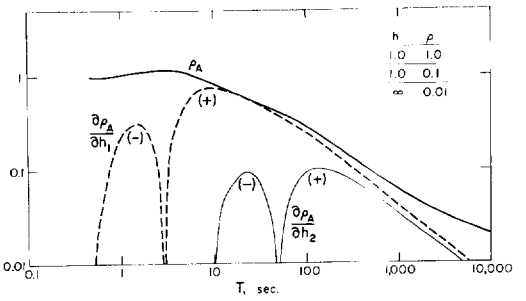

FIG. 6. Apparent resistivity and layer thickness partial derivative curves for model (1).

EXAMPLE OF INVERSION

In this section we will discuss some results of inversion of the theoretical apparent resistivity to demonstrate the power and the limitations of this scheme. They are shown in Figures 8–12 and Tables 1–5. In each figure the "observed" curve is calculated by using the models for which we have computed partials or their variations as indicated. We have also plotted the apparent resistivity curve for the initial trial model and for the first and second iterations. For the later iterations, the points are invariably hard to distinguish from the "observed" ones. These results are copied from the IBM 7094 computer on-line plots having an accuracy of 1 part in 100. For the successive iterations, the revised parameters are listed in the tables. Notice that the horizontal coordinates are unequally spaced, therefore the odd shapes of some of the curves.

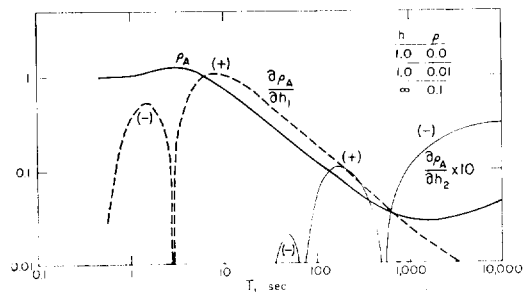

FIG. 7. Apparent resistivity and layer thickness partial derivative curves for model (3).

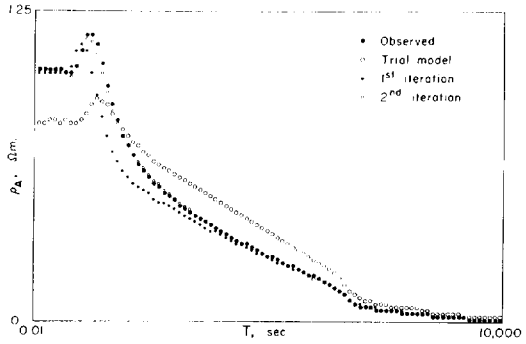

FIG. 8. Inversion of apparent resistivity curve. The "observed" curve is calculated for model (1). See Table 1 for detail of the convergence of the inversion scheme.

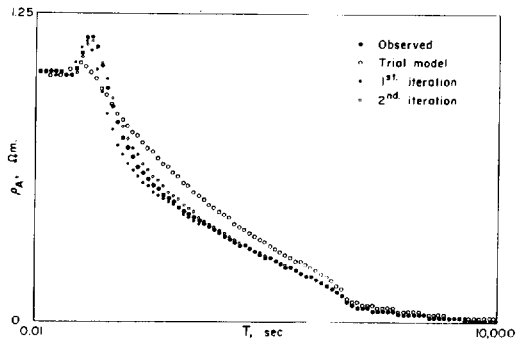

FIG. 10. Inversion of the "observed" same curve as in Figure 8. The trial model has four layers instead of three (cf. Table 3).

In Figures 8, 9, and 10 the "observed" curve was calculated by using the same model. (1) In Figure 8 the data used was from 0.01 to 10,000 sec; virtually all the features for an apparent curve were present. In this case, the convergence is seen to be very fast (Table 1), recovering within 10^{-5} of the original parameters after five iterations, even with initial parameters 20–50 percent off the correct ones. At each iteration, the curve swings from one side to another at different periods. (2) For the next case (Figure 9, Table 2), we have discarded the data for $T<8$ sec. We can see the difficulty for the program to find the topmost layer resistivity since we did not supply the short-period information to the program. Although the initial convergence is rapid, the subsequent refinement was very slow; when the first layer resistivity is sufficiently close to the correct value, the convergence becomes fast again. (3) We then tried to invert the same data as in (1) by using a four-layered model (Figure 10, Table 4) with the first layer resistivity pegged at the correct value. The convergence is more rapid than the second case, and it is interesting that $\rho_1=\rho_2=1.0$ and $h_1+h_2=1.096$, very close to the original parameters, when the time allowed (two minutes) for this computation was exceeded.

The next inversion we attempted was for the model with a low resistivity layer in the middle (Figure 11). The parameters chosen for this particular model render the layer rather opaque to the layers below for the periods considered. At 10,000 sec, the parameter resistivity was only 35 percent of the half-space resistivity. We have tried to perturb the five parameters and when the half-space resistivity was only 45 percent of the correct value, and h_2 was 100 percent off, the method failed to converge. However, when we

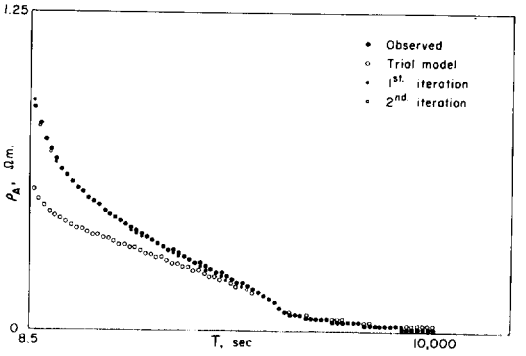

FIG. 9. Inversion of the same "observed" resistivity curve as in Figure 8, but the information for periods smaller than 8.5 sec is discarded (cf. Table 2).

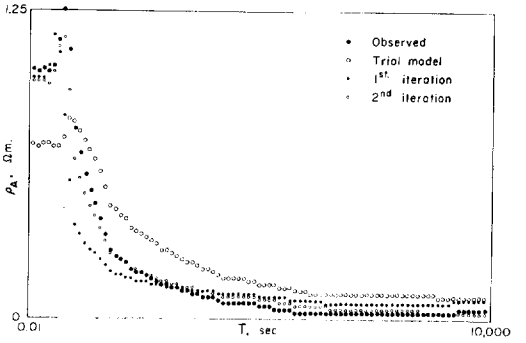

FIG. 11. Inversion of apparent resistivity curve. The "observed" curve is calculated for model (3). See Table 4 for detail.

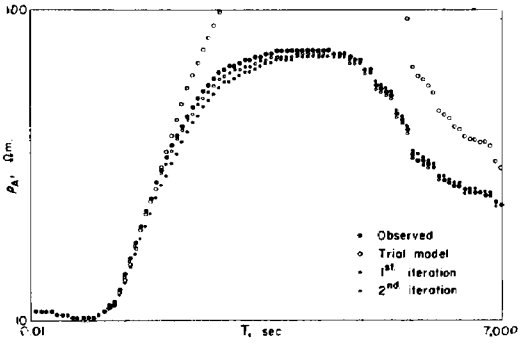

FIG. 12. Inversion of apparent resistivity curve. The "observed" curve is calculated for the five layer model of Vozoff et al (see text).

peg the half-space resistivity, the rest of the parameters quite readily attain the correct value. This phenomenon can be predicted by looking at the partial derivative curve (Figure 4). At 10,000 sec, $\partial\rho_A/\partial\rho_3$ is increasing rapidly but is still much less than 1, and $\partial\rho_A/\partial\rho_2$ still dominates; the apparent resistivity curve does not contain enough information for the half-space.

Finally we look at the more realistic five-layered model. Our main aim here is to see whether we can determine the thickness of the high resistivity layer. We pegged five of the nine parameters and the result (Table 4, Figure 12) shows that reasonable figures were attained after six trials.

The numerical experiments in this section show that the method we used works satisfactorily with theoretically calculated "observations." We can make the following comments: (1) The short period data is needed for fast convergence of the inversion. However, we can find the correct structure, though slowly, using data beyond the point where the apparent resistivity curve starts to show the influence of the lower layers. (2) A strategy for better fitting would be the use of large numbers of layers for the trial model. The inversion process would merely make the layer resistivity the same. If there are fewer layers than needed, the process may not converge to the limit desired.

As in other branches of geophysics, the interpretation would improve greatly in accuracy and speed if we had auxiliary data such as seismic information; laboratory resistivity measurements of common rocks; and for deep sounding, measurements under high temperature and pressure to delimit our initial guesses.

CONCLUSION

The inversion method used in this work is sufficiently general. Most of the layered media problems in electrical or electromagnetic sounding can be inverted in this manner. This method eliminates part of the labor in finding the parameters of a model that yield the best fit and enables us to use more layers, hence to extract the maximum information from the data. Master

Table 1. Convergence of the inversion for model (1)

	ρ_1	h_1	ρ_2	h_2	ρ_3	S.E.
Trial	0.8	1.3	0.15	1.2	0.015	1.08×10^{-1}
1st	.993	.788	.164	1.23	0.0126	6.00×10^{-2}
2nd	.992	1.05	.123	.952	0.0133	9.00×10^{-3}
3rd	.999	1.11	.0961	.980	0.0104	2.60×10^{-3}
4th	1.00	1.10	0.10	1.00	0.00999	2.05×10^{-5}
Final	1.00	1.10	0.100	1.00	0.0100	3.41×10^{-6}

Table 2. Convergence of the inversion for model (1); information for periods shorter than 8.5 sec discarded

ρ_1	h_1	ρ_2	h_2	ρ_3	S.E.
.800	.700	.15	1.3	.015	0.9×10^{-1}
1.43	.956	.119	1.08	.0109	0.5×10^{-2}
1.28	.971	.123	1.08	.0108	0.18×10^{-2}
1.24	.983	.121	1.07	.0107	0.14×10^{-2}
1.22	.990	.120	1.07	.0107	0.14×10^{-2}
1.20	.996	.119	1.07	.0107	0.13×10^{-2}
1.19	1.00	.117	1.06	.0106	0.12×10^{-2}
1.17	1.01	.116	.106	.0106	0.12×10^{-2}
1.16	1.01	.115	.105	.0105	0.11×10^{-2}
1.15	1.02	.114	.105	.0105	0.10×10^{-2}
1.14	1.02	.113	.104	.0105	0.95×10^{-3}
1.06	1.06	.107	.102	.0103	0.89×10^{-3}
.995	1.10	.100	.0999	.0100	0.32×10^{-5}
1.00	1.10	.100	.100	.0100	0.74×10^{-7}

Table 3. Convergence of the inversion for model (1) with four layer trial model

	ρ_1	1	ρ_2	h_2	ρ_3	h_3	ρ_4	SE
Trial	1.0	0.7	0.5	0.7	0.15	0.8	0.015	0.7×10^{-1}
1st	1.0	0.908	.413	.480	.134	1.11	.0106	0.3×10^{-1}
2nd	1.0	0.969	+.516	.224	.0985	.888	.0186	0.2×10^{-1}
3rd	1.0	0.989	+.511	.123	.100	.983	.0101	0.13×10^{-2}
4th	1.0	0.989	+.654	.118	.0993	.994	.00995	0.73×10^{-3}
5th	1.0	0.097	+.863	.114	.0999	1.00	.00999	0.61×10^{-3}
6th	1.0	0.986	+.983	.114	.100	1.00	.0100	0.87×10^{-4}
Final	1.0	0.986	+1.10	.114	.100	1.00	.0100	0.12×10^{-6}

Table 4. Convergence of the inversion or model (3)

ρ_1	h_1	ρ_2	h_2	ρ_3	SE
0.7	1.3	0.05	1.20	0.10	1.50×10^{-1}
0.974	0.530	0.0611	4.39	0.10	1.12×10^{-1}
0.953	0.865	0.0291	6.83	0.10	3.56×10^{-2}
0.959	0.872	0.0287	5.48	0.10	3.36×10^{-2}
0.982	0.910	0.0243	2.23	0.10	2.30×10^{-2}
0.999	0.979	0.0125	1.44	0.10	5.11×10^{-3}
1.00	0.999	0.0100	0.926	0.10	1.29×10^{-3}
1.00	1.00	0.0100	0.996	0.10	7.13×10^{-5}
1.00	1.00	0.0100	1.00	0.10	3.55×10^{-7}

Table 5. Convergence of the inversion for the five layer model of Vozoff et al (see text)

ρ_1	h_1	ρ_2	h_2	ρ_3	h_3	ρ_4	h_4	ρ_5	SE
13	2.31	100	1.29	10	0.5	10^7	50	30	2.17×10^{-1}
13	2.31	147	1.29	8.98	0.573	10^7	32.4	30	2.4×10^{-0}
13	2.31	263	1.29	9.84	0.545	10^7	30.8	30	9.10×10^{-1}
13	2.31	132	1.29	10.3	0.51	10^7	30.9	30	6.00×10^{-1}
13	2.31	144	1.29	10.4	.496	10^7	30.9	30	1.39×10^{-2}
13	2.31	144	1.29	10.3	.490	10^7	30.9	30	2.90×10^{-3}

curves are still useful in finding the approximate structure for the initial guesses, but we need only a very limited number of them. The uniqueness of the interpretation cannot be guaranteed. Where the partial derivatives for a structure are linearly independent, we could expect the inversion to be unique in a local sense, that is to say, if our initial guesses are not too far from the correct values. So far, we have only tried the method on theoretical "data"; large numbers of field-data trials will determine further the capability of this method.

ACKNOWLEDGMENT

This research was supported by the Air Force Office of Scientific Research, Office of Aerospace Research, United States Air Force, under AFOSR contract number AF-49(638)-1337.

REFERENCES

Anderson, D. L., 1966, Recent evidence concerning the structure and composition of the earth's mantle, *in* Physics and chemistry of the earth, p. 1–131: Oxford and New York, Pergamon Press.

Archambeau, C., and Anderson, D. L., 1963, Inversion of surface wave dispersion data: Publication du Bureau Central Sismologique International Serie A, Travaux Scientifiques, Fascicule 23, p. 45–54.

Backus, G. E., and Gilbert, V. F., 1967, Numerical application of a formalism for geophysical inverse problem: Geophys. J., R. Astr. Soc., v. 13, p. 247–276.

Cagniard, L., 1953, Basic theory of the magneto-telluric method of geophysical prospecting: Geophysics, v. 18, 605–635.

Cantwell, T., and Madden, T. R., 1960, Preliminary report on crustal magnetotelluric measurements: J. Geophys. Res., v. 65, p. 4202–4205.

Dorman, J., and Ewing, M., 1962, Numerical inversion of seismic surface wave dispersion data and crust-mantle structure in the New York-Pennsylvania area: J. Geophys. Res., v. 67, p. 5227–5241.

Haskell, N. A., 1953, The dispersion of surface waves on multilayered media: Bull. Seismol. Soc. Am., v. 52, p. 321–332.

Madden, T. R., and Nelson, P., 1964, A defense of Cagniard's magnetotelluric method: ONR Project NR-371–401, Geophys. Lab., M.I.T.

Margenau, H., and Murphy, G. M., 1943, The mathematics of physics and chemistry: Princeton, D. Van Nostrand Co.

Marquardt, D. W., 1963, An algorithm for least squares estimation of nonlinear parameters: J. Soc. Indust. Appl. Math., v. 11, p. 431–441.

Price, A. T., 1962, The theory of magnetotelluric methods when the source field is considered: J. Geophys. Res., v. 67, p. 1907–1918.

Swift, C. M., 1967, A magnetotelluric investigation of an electrical conductivity anomaly in the South-

western United States: Thesis, Massachusetts Institute of Technology.
Vozoff, K., 1958, Numerical resistivity analysis: Horizontal Layers: Geophysics, v. 23, p. 536–556.
———Ellis, R. M., and Burke, M. D., 1964, Telluric currents and their use in petroleum exploration: Bull. Am. Assoc. Petrol. Geol., v. 48, p. 1890–1901.
Wait, J. R., 1954, On the relation between telluric currents and the earth's magnetic field: Geophysics, v. 19, 281–289.
Yungul, S. H., 1961, Magnetotelluric sounding three layer interpretation curves: Geophysics, v. 26, p. 465–473.